

Optimized data analysis for the assessment of aortic pressure difference maps

J. Bock¹, A. Frydrychowicz¹, K. M. Johnson², O. Wieben², J. Hennig¹, and M. Markl¹

¹Diagnostic Radiology, Medical Physics, University Hospital Freiburg, Freiburg, Germany, ²Medical Physics, University of Wisconsin, Madison, WI, United States

Introduction: Time-resolved (CINE) 3-directionally encoded phase contrast (PC) 3D MRI (flow sensitive 4D MRI) techniques have been successfully applied for the analysis of vascular hemodynamics¹. The acquired data can be used for analysis of blood flow as well as to calculate additional information on vessel geometry such as time-averaged 3D PC-MRA². The derived vessel boundaries are useful for calculation of further hemodynamic parameters such as wall shear stress or pressure gradients. Cardiovascular pressure gradients are an important clinical marker for the evaluation of the severity of disease. Previous studies were limited regarding coverage of the vessel of interest by either relying on data from 2D slices³ or by calculating pressure gradients along predefined pathways^{4,5}. More recently, true 3D pressure difference (PD) mapping based on radial 3D CINE PC-MRI has been reported and applied in different vascular territories in animal studies^{6,7}. To our knowledge only in the original research by Tyszka et al. at time-resolved 3D pressures differences in the aorta in one healthy volunteer⁸ have been reported so far. However, no systematic study including quantitative analysis and visualization of the spatial and temporal distribution of time-resolved 3D pressure differences in the human aorta has been presented to date. It was therefore the purpose of this study to evaluate the potential of an optimized data analysis strategy for the assessment of aortic PD maps. The comprehensive information available in flow sensitive 4D MRI data was used to derive a segmented aortic lumen and registered PD maps from the same data set.

Methods: After ethical approval and informed consent 12 healthy volunteers (mean age 24.5) and 4 patients (mean age 23.8) with aortic coarctation were included in our study. Flow sensitive 4D MRI measurements covering the entire thoracic aorta were performed using a respiration controlled and ECG-gated rf-spoiled gradient echo sequence (spatial resolution 1.9-2.4 x 1.7-1.8 x 2.0-2.5mm³, temporal resolution 39.2- 40.8 ms, venc=150-230 cm/s) on a 3T system (Magnetom Trio, Siemens AG, Germany, standard 8-channel phased-array surface coil).

Data analysis: For automated 3D pressure difference estimation a reliable identification of the aortic lumen was required. Therefore a processing chain including PC-MRA calculation, thresh-holding and a flood fill algorithm was implemented as shown in fig.1. Time-averaged PC-MRA was calculated using the absolute velocity combined with noise masking, static tissue removal, and magnitude weighting⁹ (Eq. in fig.1). For subsequent calculation of pressure gradients, the aortic lumen had to be separated from the pulmonary system, which was achieved by simple thresholding. In some cases morphological operations had to be applied to break the connectivity between aorta and pulmonary system and to close holes in the objects. To ensure inter-subject comparability of the data, a reference point (PD = 0), was marked manually at the height of lower edge of the pulmonary artery (s. fig.2). Next, the reference point was used to initiate the flood fill algorithm to generate a 3D binary mask containing only voxels within the aortic lumen. This mask was used in conjunction with 4D velocity data to derive time-resolved pixel-wise 3D pressure differences, which were calculated independently for each time frame. In the first step pressure gradients were calculated using the Navier-Stokes equation assuming Newtonian fluid, viscosity 3.2e⁻³ Pa·s, density 1060.0 kg/m³. Based on pressure gradients, pressure differences were calculated and then iteratively refined similar to the methods reported by Tyszka et al.⁸. For quantitative data comparison 5 analysis planes were placed at different anatomical landmarks (above the reference point in the AAO, before first aortic branch, after last aortic branch, at the height of reference point in the DAA and 5cm further downstream in the DAA, s. Fig. 2). In patients' data 2 additional analysis planes before and after the anastomosis were placed. Mean and peak pressure differences were calculated in each plane for each time frame.

Results: Mean pressure differences over 12 volunteers in 5 analysis planes are shown as mean ± standard deviation in fig. 2. High systolic pressure difference (mean PD between AAO and DAAII = -9.6 ± 3.4 mmHg) and reflected pressure wave, i.e. inverted pressure difference (mean PD between AAO and DAAII = 4.2 ± 2.2 mmHg) during early diastole, were clearly visible in all volunteers. Magnitude and range of normal aortic pressure differences were in good agreement with literature values^{4,8}. Note the relatively small standard deviations in fig. 2 indicate high data consistency between volunteers. To validate our PD mapping approach, pressure gradients across the site of aortic coarctation as determined by the reference standard echocardiography were compared to MRI findings at the same location (table 1). In 2 cases calculated pressure gradients showed excellent agreement while MRI underestimated PD differences in the 2 remaining patients. Fig. 3 illustrates the potential of the method for the comprehensive assessment of the hemodynamic status of the aorta including 3D blood flow visualization, 3D PD maps, and local PD curve derived from a single data set.

Discussion: The study demonstrated the feasibility of the proposed processing strategy for the derivation of a time-averaged aortic segmentation from flow sensitive 4D MRI. The determined vessel lumen could successfully be used to automatically derive time-resolved 3D pressure difference maps. However, the currently applied algorithms can only identify the inner part of the aortic lumen and do not provide the exact location of the aortic walls. Nevertheless, pressure differences inside the detected lumen could still be reliably estimated as indicated by the consistent data and good agreement with echocardiography. Future work will focus on the derivation of more accurate time-resolved segmentation and the calculation of further hemodynamic parameters such as pulse wave velocity.

Acknowledgements: Deutsche Forschungsgemeinschaft (DFG), Grant # MA 2383/4-1, Bundesministerium für Bildung und Forschung (BMBF), Grant # 01EV0706.

References

- [1] Markl M, et al. JMRI 2007;25
- [2] Dumoulin CL. Magn Reson Imaging Clin N Am 1995; 3
- [3] Thompson RB, et al. MRM 2003;49
- [4] Ebberts T, et al. MRM 2001;45
- [5] Nagao T, Magn Reson Med Sci 2008;7
- [6] Lum DP, et al. Radiology 2007;245
- [7] Mofattkhar R, et al. AJNR 2007;28
- [8] Tyszka M, JMRI 2000;12
- [9] Bock J., Proc. ISMRM 2007; p 3138

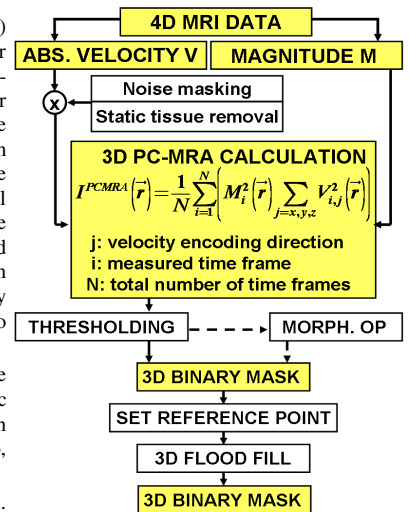


Fig. 1 Process chain for PC-MRA calculation

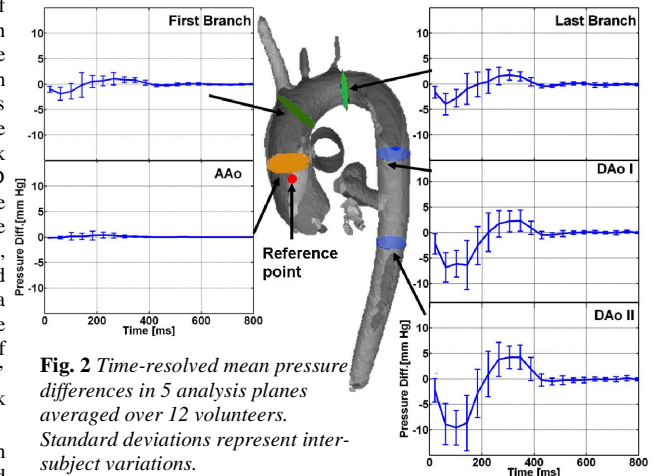


Fig. 2 Time-resolved mean pressure differences in 5 analysis planes averaged over 12 volunteers. Standard deviations represent inter-subject variations.

Patients	Pmax [mmHg]	
	echo	PD maps
1	19	6,8
2	29	28,5
3	37	38,6
4	17,1	10

Tab. 1 Comparison of pressure gradients across the stenosis between echocardiography and PD maps calculated from MRI.

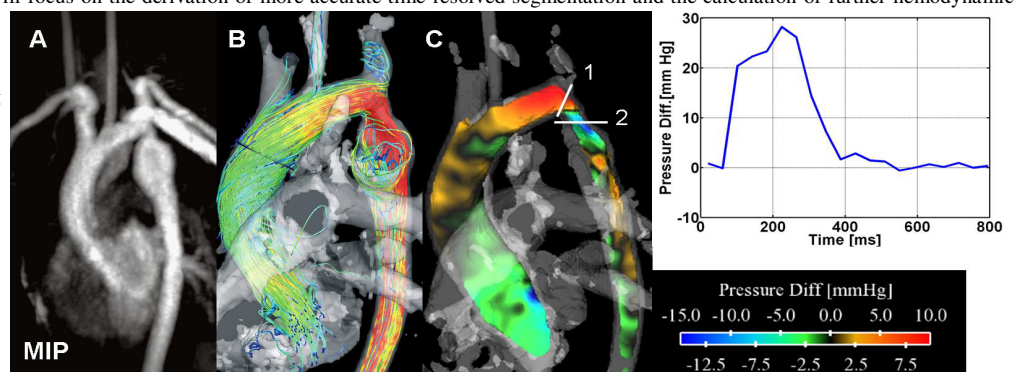


Fig. 3 Results for one patient with aortic coarctation for a systolic time frame a) CE-MRA, b) 3D streamlines c) 3D systolic pressure differences directly mapped onto the aorta. Top, right: time-resolved peak pressure gradient between planes 1 and 2